

See discussions, stats, and author profiles for this publication at: <https://www.researchgate.net/publication/265913825>

Conjugated Polymer Nanoparticles by Suzuki-Miyaura Cross-Coupling Reactions in an Emulsion at Room Temperature

ARTICLE in MACROMOLECULES · OCTOBER 2014

Impact Factor: 5.8 · DOI: 10.1021/ma501402h

CITATIONS

5

READS

97

9 AUTHORS, INCLUDING:



Ming-Tsz Chen

The University of Manchester

31 PUBLICATIONS 333 CITATIONS

[SEE PROFILE](#)



Oscar Navarro

University of Sussex

76 PUBLICATIONS 2,809 CITATIONS

[SEE PROFILE](#)



Vinich Promarak

Vidyasirimedhi Institute of Science and Techn...

98 PUBLICATIONS 1,426 CITATIONS

[SEE PROFILE](#)



michael L Turner

The University of Manchester

153 PUBLICATIONS 2,900 CITATIONS

[SEE PROFILE](#)

Conjugated Polymer Nanoparticles by Suzuki–Miyaura Cross-Coupling Reactions in an Emulsion at Room Temperature

Duangratchaneekorn Muenmart,^{†,‡} Andrew B. Foster,^{*,†} Alan Harvey,^{‡,¶} Ming-Tsz Chen,^{†,#} Oscar Navarro,[§] Vinich Promarak,[△] Mark C. McCairn,[†] Jonathan M. Behrendt,[†] and Michael L. Turner^{*,†}

[†]School of Chemistry, University of Manchester, Oxford Road, Manchester M13 9PL, U.K.

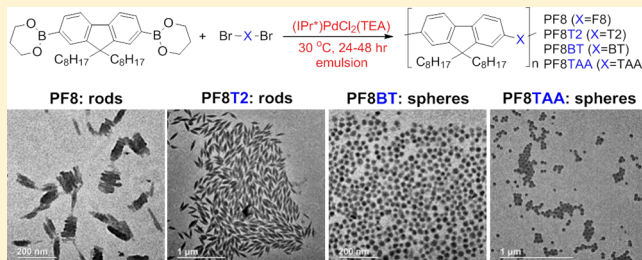
[‡]School of Materials, University of Manchester, Manchester M1 7HS, U.K.

[§]Department of Chemistry, University of Sussex, Brighton BN1 9QJ, U.K.

[△]School of Chemistry and Center of Excellence for Innovation in Chemistry, Institute of Science, Suranaree University of Technology, Nakhon Ratchasima, 30000 Thailand

Supporting Information

ABSTRACT: A range of stable emulsions of spherical and rod-like conjugated polymer nanoparticles (CPN) were synthesized via Suzuki–Miyaura cross-coupling reactions of 9,9-dioctylfluorene-2,7-diboronic acid bis(1,3-propanediol) ester with a number of different dibromoarene monomers in xylene, stabilized in water by the nonionic surfactant, Triton X-102. High molar mass poly(9,9-dioctylfluorene) (PF8), poly(9,9-dioctylfluorene-*alt*-benzothiadiazole) (PF8BT), poly(9,9-dioctylfluorene-*alt*-4-sec-butylphenyldiphenylamine) (PF8TAA) and poly(9,9-dioctylfluorene-*alt*-bithiophene) (PF8T2) emulsions were obtained, at high overall conjugated polymer concentrations (up to 11,000 ppm), in the presence of the palladium complex, (IPr*)PdCl₂(TEA) and base, tetraethylammonium hydroxide, in nitrogen atmosphere at 30 °C after 24–48 h. TEM analysis of the PF8 and PF8T2 emulsions revealed regular rod-like structures, up to 200 nm in length with aspect ratios of 4–5. PF8BT and PF8TAA formed spherical particles with diameters of between 20–40 nm in TEM analysis. UV–vis absorption spectra of the PF8 emulsions indicated high levels of ordered β-phase configuration (9–10%) in their respective nanoparticles. Absolute photoluminescence quantum yields (Φ) of 21–25% were recorded for these emulsions.



INTRODUCTION

Nanoparticles of conjugated polymers (CPNs) show many attractive features for biomedical, photonic and electronic applications. Current interest in the use of fluorescent CPNs in nanomedicine, e.g., *in vivo* and *in vitro* imaging and fluorescence-based biosensing, is driven by their high brightness, excellent photostability, high quantum yields, low cytotoxicity, and potential for surface modification.^{1–3} The semiconducting and emissive properties of the constituent polymers have also led to their widespread application as the active layer in organic electronic devices, such as organic light emitting diodes (OLEDs), organic field effect transistors (OFETs), and organic photovoltaics (OPVs). The use of CPNs in device fabrication has increasingly been explored due to the associated promise of low temperature processing techniques from an environmentally benign solvent (water). Moreover, even relatively insoluble conjugated polymers can be prepared as stable aqueous dispersions of nanoparticles, in which they show much lower viscosities than the equivalent loadings of high molar mass conjugated polymer dissolved in organic solvents. Aqueous-based inks are therefore attractive alternatives for commercial production of these devices by printing.^{4–7}

Previous work on the preparation of CPNs has largely focused on the formulation of preformed conjugated polymers into nanoparticle dispersions, e.g., via reprecipitation,^{8–10} mini-emulsion,^{11–14} or self-assembly.¹⁵ Polymerization with concurrent formation of nanoparticles has been less extensively studied, but provides the promise of a direct, scalable approach to CPNs.^{16–18} Initial reports described a nonaqueous emulsion process using block copolymers as stabilizers,¹⁶ and more recently aqueous dispersions of small nanoparticles (<30 nm) were prepared by a Glaser coupling in a mini-emulsion system.¹⁷ Larger hyperbranched nanoparticles, ca. 200 nm diameter, have been synthesized by Suzuki–Miyaura cross-coupling reactions in a modified emulsion polymerization at 90 °C using a nonionic surfactant from the Tween series.¹⁸ In general the Suzuki–Miyaura coupling reaction is the method of choice for the preparation of high molecular weight conjugated polymers as it avoids the use of highly air sensitive or exceptionally toxic organometallic reagents and the byproducts can be easily removed.¹⁹ However, using conventional catalysts

Received: July 8, 2014

Revised: August 22, 2014

Published: September 18, 2014

this reaction is generally carried out at temperatures $>80\text{ }^{\circ}\text{C}$, a temperature at which most nonionic surfactants are above their cloud point at the concentrations required to stabilize an emulsion of the initial organic phase (monomers and solvent). Ionic surfactants such as sodium dodecyl sulfate (which typically have much higher cloud points than their nonionic counterparts) have been successfully used in a Suzuki–Miyaura coupling miniemulsion reactions at high temperature ($90\text{ }^{\circ}\text{C}$).²⁰ However, the disadvantage of the use of ionic over steric stabilization, is that the resultant particles will be sensitive to changes in ionic strength and are therefore more likely to flocculate in a physiological environment. Improved catalysts that facilitate Suzuki–Miyaura cross-coupling polymerization at lower temperatures are required for compatibility with the majority of nonionic surfactants. We have recently reported suitable catalysts based on (*N*-heterocyclic carbene)-PdCl₂(triethylamine) complexes.^{21–23} These complexes are moisture stable and can effectively catalyze the Suzuki–Miyaura reaction at room temperature.²¹

The complex relationship between order, disorder, aggregation and the optoelectronic properties of conjugated polymers has been extensively investigated as it underpins the performance of these polymers in devices.^{24–26} The photophysical properties of conjugated polymers dispersed as nanoparticles have been less intensely examined. In general they consist of isolated polymer chains but nanoparticle formation can also induce aggregation of polymer chains and ordered conformations. For instance McNeill and Wu reported that solvent-induced swelling of polyfluorene nanoparticles led to increased planarization of the polymer chains to yield a significant proportion of the more extended β -phase conformation,²⁷ resulting in an increased quantum yield for these CPNs.²⁸ We have recently demonstrated several strategies that can be used to control the β -phase content of PFO-based nanoparticles, involving either substitution of a proportion of the octyl side chains with oligo(ethylene glycol)²⁹ or by incorporation of the conjugated polymer into a covalent nanocomposite with silica.³⁰

Within the field of organic electronics, thin films of PQT12 deposited from nonaqueous dispersions of nanoparticles have been shown to display higher crystallinity than films deposited from PQT12 dissolved in a good solvent, leading to improved OFET performance.³¹ The morphology of the nanoparticles prepared in previous studies has generally been spherical, even when the polymer chains are aggregated. Isolation of anisotropic nanoparticles significantly extends the range of nanostructures available and can control the photonic band gap of colloidal crystals.³² Previous work has shown that ellipsoidal polymer nanoparticles can be isolated by annealing of ordered structures of PF8 and PF8BT³³ or by stretching large particles of PF8BT dispersed in a PVA matrix while heating above the T_g of the conjugated polymer.³²

In this contribution we report the room temperature synthesis of stable dispersions of conjugated polymer nanoparticles by the Suzuki–Miyaura cross-coupling of 9,9-dioctylfluorene-2,7-diboronic acid *bis*-(1,3-propanediol) ester (**1**) with a range of dibromo arenes (**2–5**) (structures displayed in Chart 1). High concentrations (up to 11 mg mL^{-1}) of conjugated polymers such as poly(9,9-dioctylfluorene) (PF8), poly(9,9-dioctylfluorene-*alt*-benzothiadiazole) (PF8BT), poly(9,9-dioctylfluorene-*alt*-4-s-butylphenylidiphenylamine) (PF8TAA) and poly(9,9-dioctylfluorene-*alt*-bithiophene) (PF8T2) (Chart 2) can be isolated directly from the reaction.

Chart 1. Structures of Monomers (1–5) and Complex (6) Used in the Suzuki–Miyaura Cross-Coupling Polymerization Reactions to Produce Stable Dispersions of Conjugated Polymer Nanoparticles

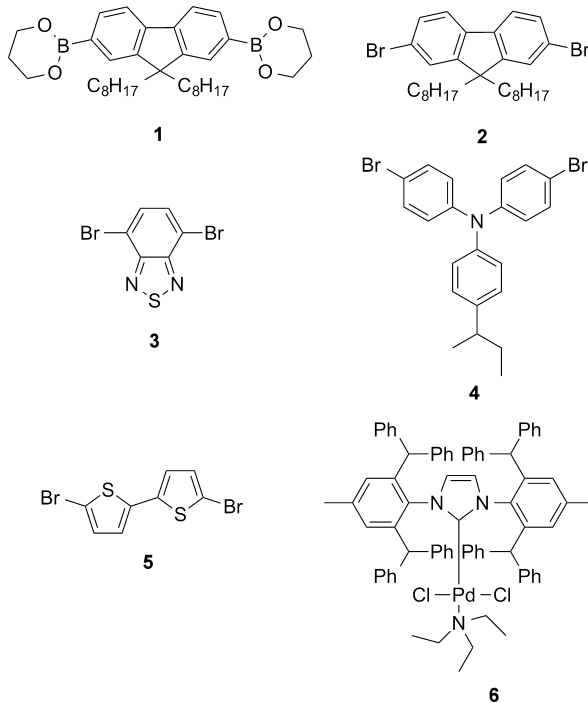
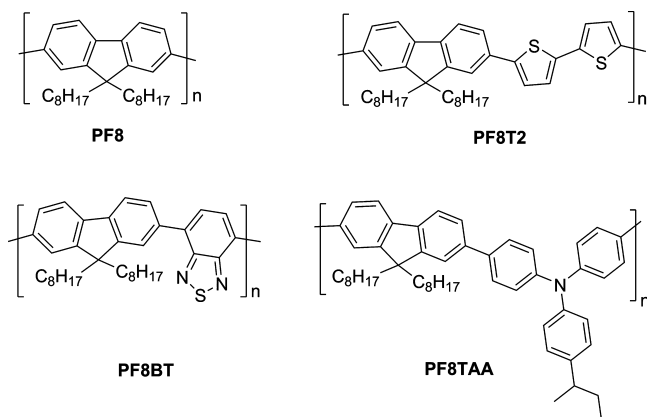


Chart 2. Structures of Polymers Produced in Low Temperature Suzuki–Miyaura Cross-Coupling Polymerizations



While PF8BT and PF8TAA form spherical CPNs, PF8 and PF8T2 are almost exclusively observed as homogeneous dispersions of rod-like nanoparticles. This unprecedented self-assembly, which occurs during the polymerization reaction, provides high concentrations of anisotropic nanoparticles with useful photophysical and semiconducting properties.

EXPERIMENTAL SECTION

Materials. Monomers (**1–3**, **5**), tetraethylammonium hydroxide (40% in water), xylene and Triton X-102 surfactant were purchased from Aldrich Ltd. and used as supplied. The triarylamine monomer (**4**), *N,N*-bis(4-bromophenyl)-4-(1-methylpropyl)-benzeneamine, was kindly supplied by Cambridge Display Technology Ltd. The complex, (PdCl₂)(PPh₃)₂ (TEA) (**6**) was synthesized using a published method.²² A metal scavenger resin, SiliaMetS DMT (dimercaptotriazine) 40–

Table 1. Suzuki–Miyaura Cross-Coupling Polymerizations of Diboronic Ester Monomer (1) with Dibromo Monomers (2–5) under Different Emulsion Conditions To Produce PF8, PF8BT, PF8TAA, and PF8T2^a

reaction	monomers, 1 + x	total monomer/mmol	xylene, y/mL	Triton X-102, z/wt %	polymer concn ^b /mg mL ⁻¹	molar mass ^c /kg mol ⁻¹	particle size/nm			
							DLS ^d	TEM ^e	d_z [PDI]	
A	2	0.4	2	5	PF8, 3.0	27.2	87.5	53 [0.33]	21	76, 18 r
B	2	0.8	2	5	PF8, 6.0	28.9	95.4	55 [0.41]	26	74, 16 r
C	2	1.2	4	10	PF8, 8.6	6.1, 48. ^f	7.3, 83. ^f	81 [0.32] ^f	22 ^f	99, 23 r
D	2	1.6	6	15	PF8, 11.1	12.9	39.4	88 [0.22]	41	106, 25 r
E	3	0.4	2	5	PF8BT, 2.0	24.2	82.7	33 [0.20]	21	23 s
F	3	0.8	2	5	PF8BT, 4.0	26.0	67.1	34 [0.16]	23	22 s
G	4	0.4	2	5	PF8TAA, 2.6	18.5	49.8	41 [0.33]	18	19 s
H	4	1.6	8	20	PF8TAA, 9.5	9.2	21.7	56 [0.22]	33	41 s
I	5	0.4	2	5	PF8T2, 2.1	12.1	32.7	61 [0.34]	23	82, 18 r
J	5	1.6	4	10	PF8T2, 8.2	12.7	36.1	88 [0.18]	35	205, 52 r

^aReaction conditions: equimolar quantities of monomers, 1 + x, dissolved in y mL of xylene; 50 mL of z wt % Triton X-102 solution; 1 equiv mmol of tetraethylammonium hydroxide; 2 mol % of (IPr*)PdCl₂(TEA) complex (6); 30 °C; typically 24 h, 48 h for reactions G and H. ^bApproximately conjugated polymer concentration of emulsion upon complete conversion. ^cDetermined by GPC in THF vs polystyrene standards. ^dDLS analysis of the z-average and number-average particle (d_z and d_n) sizes of emulsion particles at 25 °C; polydispersity index (PDI) of particles presented. ^eTEM analysis of the number-average length (l_n) and number-average width (w_n) dimensions or the number-average particle (d_n) sizes of emulsion nanoparticles (d_n), denoted with s: predominantly spherical or r: predominantly rod-like in shape. Averages were determined from the measurement of at least 100 nanoparticles in each case. ^fMolar masses of resolved bimodal distribution of peaks observed in GPC trace of reaction C, presented in Figure 2. Number-average particle size (d_n) distribution was also bimodal for this emulsion.

63 μm, 60 Å, was purchased from Crawford Scientific Ltd. to remove palladium from the resultant dispersions.

Typical Polymerization Reaction. The following procedure was used to produce a nanoparticulate PF8 dispersion, designated as reaction A in Table 1. Tetraethylammonium hydroxide solution (40% in water) (0.16 g, 0.4 mmol) was added to an aqueous solution (50 mL) of nonionic surfactant, Triton X-102 (2.5 g, 5 wt % in deionized water) in a 100 mL three necked round-bottom flask. The contents were then thoroughly degassed for 30 min by bubbling nitrogen gas through the solution, while being stirred using a D-shaped PTFE paddle powered by an overhead stirrer motor. Then a separate 10 mL two necked round-bottom flask was used to mix together the monomers in the organic solvent prior to addition to the reaction flask: Monomer 1 (0.1151 g, 0.2 mmol) and monomer 2 (0.1096 g, 0.2 mmol) were dissolved in xylene (2 mL). The monomer solution was degassed and then the complex (IPr*)PdCl₂(TEA) (0.0095 g, 0.008 mmol) was added, followed by further degassing of the resultant solution. A syringe was used to transfer the monomer/catalyst solution into the stirring surfactant/base solution (300 rpm) in the main reaction flask now maintained at 30 °C. The contents were mechanically stirred under nitrogen gas at 30 °C for 24 h. The addition of the monomer/catalyst mixture causes the contents to become cloudy. After about 1 h, the reaction contents cleared as the nanoparticles formed and the color of the dispersion progressively changed to pale yellow over the remaining reaction time.

Characterization. The molar mass of the conjugated polymer produced in each reaction was analyzed using gel permeation chromatography (GPC). GPC of the conjugated polymers recovered from the dispersions was completed in tetrahydrofuran (THF) [1–2 mg mL⁻¹] at 35 °C using a Viscotek GPCmax VE2001 solvent/sample module with 2 x PL gel 10 μm mixed-B and a PL gel 500 A column, a Viscotek VE3580 RI detector and a VE3240 UV/vis multichannel detector. The injection volume was 100 μL and the flow rate was 1 mL min⁻¹. The system was calibrated with low polydispersity polystyrene standards, in the range 200 to 6 × 10⁶ g mol⁻¹, from Agilent Technologies, with results analyzed using Malvern Omnisec software. Particle size analysis of the dispersions was completed using both dynamic light scattering (DLS) and transmission electron microscopy (TEM).

The particle size distributions of diluted samples were measured at 25 °C using a Malvern Zetasizer Nano ZS (DLS). The DLS results

quoted are the average of three measurements. TEM analysis was completed using a FEI Tecnai 20 instrument working at 80 kV. Diluted samples containing approximately 100 ppm conjugated polymer concentrations were drop cast on to Formvar coated, 3 mm 400 mesh copper grids (produced by Agar Scientific). The images were taken in standard diffraction contrast. The particle size analysis of the images was completed using ImageJ software. Polymer samples were recovered from the dispersions and were dissolved in THF to a concentration of 10 mg mL⁻¹ for MALDI analysis. A similar solution was prepared of the matrix (dithranol). The dithranol was dissolved in THF to a concentration of 10 mg mL⁻¹. One μL of polymer sample solution was mixed with 10 μL of matrix solution. The solution was mixed and approximately 0.5 μL was spotted onto the MALDI plate. UV-vis absorption spectra were recorded on a Varian Cary 5000 UV-vis-NIR spectrophotometer, either diluted in water (nanoparticles) or dissolved in THF (polymer) at room temperature. Photoluminescence spectra were recorded on a Varian Cary Eclipse fluorimeter, either diluted in water (nanoparticles) or dissolved in THF (polymer). All absolute photoluminescence quantum yield (PLQY, Φ) measurements were obtained using a Fluoromax-4 spectrofluorometer with integrating sphere attachment (instrument standardized with a tungsten lamp). Steps were taken to attempt to remove any palladium residues from the dispersions prior to PLQY analysis. Samples of the dispersions were first centrifuged to remove large black particles. The resultant dispersion was then treated overnight with excess metal scavenger exchange resin (×8 amount of suspected palladium present in sample mixture). The resin was then removed from the emulsion via filtration through glass wool. This approach proved unsuccessful as ICP-MS analysis of emulsion samples treated in this manner using a Thermo Scientific iCAP 6300 Duo ICP-OES instrument indicated levels of palladium close to those originally present in the reactions. For example, in the case of reaction B this amounted to 30 ppm Pd. Nanoparticle suspensions in water were diluted to give absorption maxima values between 0.03 and 0.1, for measurements.

Background reference measurements were obtained using water (800 μL) in 7 × 40 mm clear glass vials. Nanoparticle suspensions (800 μL) were also measured in 7 × 40 mm clear glass vials. Excitation wavelengths of 380, 470, 360, and 460 nm were used for measurements of PF8, PF8BT, PF8TAA and PF8T2 respectively. As an example, to calculate PLQYs of the PF8 emulsion samples, four measurements were obtained in each case: (i) background scatter

(370–390 nm); (ii) background fluorescence (390–750 nm); (iii) sample scatter (370–390 nm); and (iv) sample fluorescence (390–750 nm). Appropriate optical filters were used to avoid oversaturation of the detector during collection of scatter measurements and these filters were corrected for in the PLQY calculation. For each sample of nanoparticles, PLQY measurements were repeated in triplicate, using a fresh suspension after each set of sample scatter and sample fluorescence measurements. The reported PLQY values are therefore an average of three PLQY measurements. Errors of 10% were typically associated with the measurements.

RESULTS AND DISCUSSION

The complex employed in this work, termed as (IPr^*)- $\text{PdCl}_2(\text{TEA})$, where IPr^* is defined as 1,3-bis[2,6-bis(diphenylmethyl)-4-methylphenyl]imidazole-2-ylidene and TEA = triethylamine, is moisture stable and can be handled in ambient atmosphere. The “throw-away” ligand, triethylamine (TEA) attached to the Pd center improves the catalyst activity as a consequence of the ease of its departure and/or the higher tendency of TEA to recoordinate to the $[(\text{NHC})-\text{Pd}(0)]$ and conserve the active species in solution. Initial experiments showed that this complex effectively catalyzes the Suzuki–Miyaura cross-coupling polymerization reactions of aryl dibromides with aryl diboronate esters at room temperature. However, the choice of boronate ester has a significant bearing on the reaction. For example, while monomer **1** (bearing 1,3-propanediol boronic acid esters) can be efficiently polymerized with an aryl dibromide **2–5** under these conditions, the corresponding boronic acid pinacol ester-functionalized monomer, produced at best oligomers in a reaction with **2** under these conditions. A possible reason for this could be the difficulty for larger pinacol ester groups to approach the metal centre in the transmetalation step, given the bulkiness of the IPr^* carbene.

Poly(9,9-dioctylfluorene) (PF8) Dispersions. Suzuki–Miyaura cross-coupling reactions were completed with equimolar amounts of monomers **1** and **2** under various conditions to produce PF8 as outlined in Table 1. The typical reaction (A) described in the Experimental Section produced PF8 polymer of high molar mass, $M_n = 27,000 \text{ g mol}^{-1}$ and a broad molar mass distribution, $M_w/M_n = 3.2$.

Dynamic light scattering (DLS) of the resultant dispersion indicated nanoparticles with a broad size distribution (polydispersity index, PDI = 0.33) exhibiting a z-average particle diameter size (d_z) of 53 nm. High PDI values (>0.2) were observed for each of the PF8 emulsions and indeed, to a lesser extent, for all of the conjugated polymer emulsions studied. In some cases this is due to the anisotropic morphology of the particles, but for spherical particles it may reflect the inability of the DLS fitting to resolve distribution(s) of small conjugated nanoparticles or a potential distribution of surfactant micelles.

Micelles of Triton X-102 surfactant exhibit a particle size diameter, d_z of 7.1 nm (PDI = 0.19) (see Supporting Information). TEM analysis of the PF8 emulsions revealed that they were predominantly composed of rod-like nanoparticles (see Figure 1) with individual rods of dimensions, $74 \times 16 \text{ nm}$ (aspect ratio of almost 5). Doubling the concentration of the two monomers (with respect to xylene) (B) did not have a significant effect on the final molar mass of PF8 polymer ($M_n = 29,000 \text{ g mol}^{-1}$) obtained. Further scale-up of the starting concentration of monomer was limited by the solubility of the monomers in xylene. Increasing the amount of xylene and surfactant (C and D) allowed higher conjugated polymer

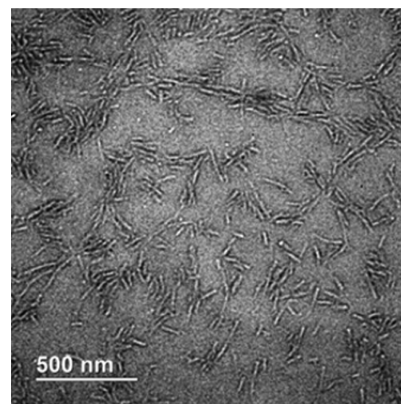


Figure 1. TEM image of surface features of PF8 emulsion (B). Individual and groups of rod-like features are present throughout the surface. Rod-like nanoparticles have dimensions of $74 (\pm 13) \text{ nm} \times 16 (\pm 2) \text{ nm}$.

content dispersions of up to 11 mg/mL to be prepared. GPC analysis of the molar mass distributions of the series of PF8 emulsion (A–D) polymers are presented in Figure 2. Polymers

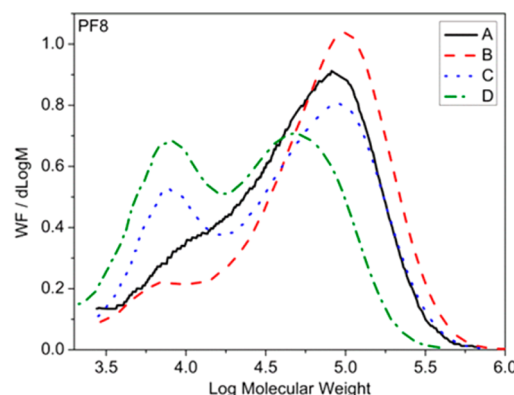


Figure 2. GPC analysis of the molar mass distributions of polymer present in the PF8 emulsions (reactions A–D in Table 1).

recovered from reactions C and D exhibited a clearly bimodal molar mass distribution. MALDI–TOF mass spectrometry of a low molar mass polymer fraction recovered from reaction C indicated that both the even and odd PF8 residue number chains were terminated almost entirely with bromine atoms: no dead ends were apparent (see Supporting Information). This indicates that homocoupling of the boronic ester fluorene monomer, **1**, must be occurring as a side-reaction, leading to lower molar masses for polymers isolated from reactions C and D. Better shear mixing may be required when the xylene to water composition is increased. However, as discussed below, comparison of the four PF8 emulsions indicates that variation in the molar mass distributions does not have a significant impact on the optical properties of the dispersion.

The largest rods of PF8 were obtained from reaction D, with dimensions measured on average at $106 \times 25 \text{ nm}$ (see Figure 3). These rods appear to aggregate into larger assemblies during sample preparation (Figure 3 right enlarged image). Recent work has indicated that evaporation of monodisperse PF8 in very dilute toluene solution leads to the formation of large lenticular crystals.³⁴ Structural analysis indicated that the polymer chains lie parallel to the long axis of the crystals and the alkyl side chains perpendicular to the substrate. The shapes

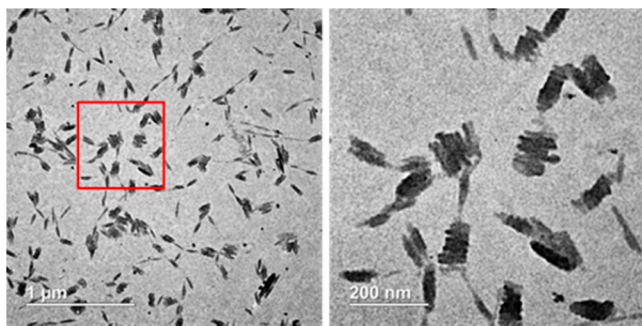


Figure 3. TEM image (left) of nanoparticles present in PF8 emulsion (D). Right image is an enlargement of area highlighted by box in left image. Predominantly rod-like particles present, with dimensions of $106 (\pm 17)$ nm $\times 25 (\pm 6)$ nm, equating to an aspect ratio of 4.

and aspect ratios of the nanoparticles reported here largely replicate those observed for micron size lenticular crystals.³³ In these crystals the polymer main chain is oriented parallel to the long axis of the crystals and if similar ordering is occurring in the PF8 dispersions shown in Figure 3 then the length of the rods is the same order of magnitude as the extended chain length of the individual PF8 molecules. A small population (5%) of spherical particles, with number-average diameter size of 27 nm, was observed by TEM.

UV-vis absorption spectra of the PF8 series (A–D) are presented in Figure 4. The main band is observed at 408 nm with a shoulder at 390 nm. Each dispersion also exhibits a significant peak at 441 nm indicating the presence of the β -phase.

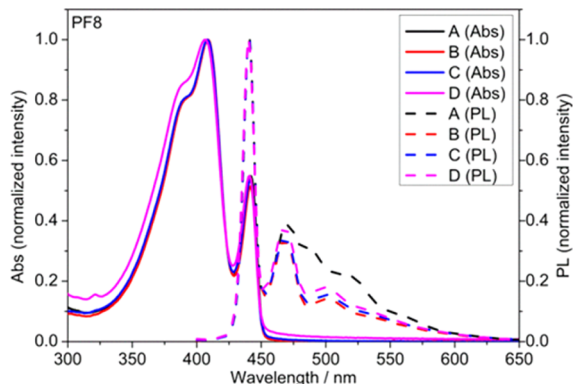


Figure 4. Absorption and photoluminescence spectra of PF8 dispersions at 20 °C (A–D).

There are no significant changes in the optical properties of the four PF8 dispersions and differences in the polymer molar mass or polymer concentration within particles do not significantly affect the proportion of β -phase present.

The percentage of β -phase present in the polymer nanoparticles was calculated at 9–10% from comparing the area of an asymmetric Gaussian peak used to fit the β -phase peak at 441 nm with a constrained multiple-Gaussian peak fitting of the broad main band attributed to the β -phase, an example for reaction A is presented in Figure 5. The vibronic replicas applied after selection of 0–0 peak in the multiple Gaussian fitting correspond to modes with energies of 85 meV (ν_1), 156 meV (ν_2) and 199 meV (ν_3), previously assigned from the β -

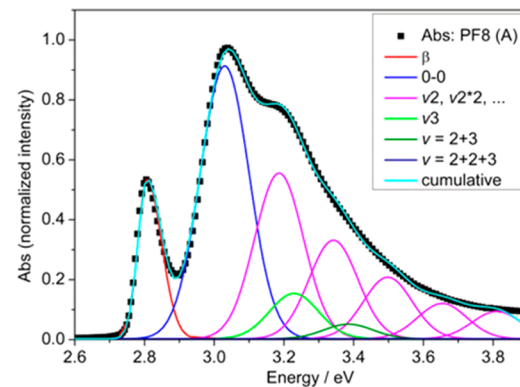


Figure 5. Area normalized absorbance of PF8 at 20 °C (reaction A) (black symbols) and the overall cumulative fit to the data (cyan solid line). The fits associated with the Gaussian spectral components 0–0 (blue) along with ν_2 (magenta) and its replicas, ν_3 (green), $\nu = (2 + 3)$ (olive) and $\nu = (2 + 2 + 3)$ (navy) and the asymmetric Gaussian fit to the β peak (red). The notation $\nu n^* m$ refers to the m th replica of the vibrational mode n .

phase PF8 photoluminescence spectrum and in agreement with that observed with Raman spectroscopy of PF8.^{36,37}

The absence of the first vibronic feature, ν_1 , which is associated with locally free chains without intermolecular contacts, again emphasizes a high level of ordering within the nanoparticles. Molar absorption coefficients at the peak maxima for the four PF8 emulsions, A to D were calculated as 38 000, 49 000, 50 000, and 44 000 $M^{-1} \text{ cm}^{-1}$ respectively. The absorption spectra of the emulsions containing xylene swollen PF8 nanoparticles closely match those previously observed for PF8 films processed from (or annealed with) similar solvents.³⁸ The dominant vibronic peaks in the emission spectra of the PF8 emulsions (Figure 4), at 440, 466, and 500 nm, are solely associated with β -phase chromophores which emphasizes the efficient energy transfer from glassy regions to the β -phase.³⁹

Larger lenticular crystals of the β -phase of preformed monodisperse PF8 have also recently been prepared from dilute *o*-dichlorobenzene solutions.³⁵ The absorption and emission spectra of the reported crystals closely match those obtained here for rod structures that are more than an order of magnitude smaller. The photoluminescence quantum yields (PLQY, Φ) were between 21–25%. These PLQY values are similar to those quoted for PF8 films containing similar levels of β -phase conformation.³⁸

Poly(9,9-dioctylfluorene-*alt*-benzothiadiazole) (PF8BT) Dispersions. Suzuki–Miyaura cross-coupling reactions with equimolar amounts of monomers **1** and **3** gave nanoparticles of PF8BT (reactions E and F, Table 1). As with the PF8 reactions (A and B), doubling the concentration of the monomers (and thus polymer) in the organic phase (2 mL) did not cause any change in the average particle size of the nanoparticles formed in the ensuing emulsions. Both reactions produced stable dispersions containing polymer of similar molar mass, $M_n = \sim 25\,000 \text{ g mol}^{-1}$ associated with nanoparticles of similar size ($d_z = 33\text{--}34 \text{ nm}$) and a homogeneous particle size distribution (PDI = 0.16–0.20). TEM of reaction E showed a uniform distribution of spherical particles with a mean particle diameter of 23 (± 6) nm, close to the number-average particle distribution indicated by DLS analysis ($d_n(\text{DLS}) = 21 \text{ nm}$, Figure 6).

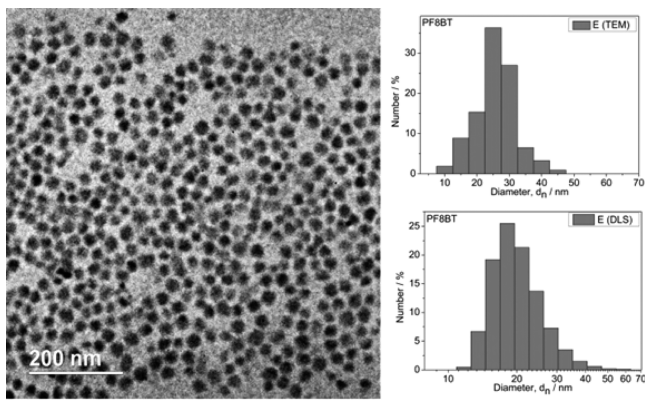


Figure 6. TEM image (left) of spherical nanoparticles present in PF8BT dispersion (E). Right images are size distribution of the particles ($d_n = 23 (\pm 6)$ nm) obtained in TEM analysis (top) compared to the number-average particle size distribution ($d_n = 21$ nm) of the dispersion obtained in DLS analysis (bottom).

MALDI-TOF mass spectrometry of a low molar mass polymer fraction of the PF8BT emulsions indicated only structures terminated with bromine atoms: no dead ends were apparent (see Supporting Information) but a fraction of the low molar mass chains are unexpectedly rich in F8 units suggesting that some homocoupling of the boronic ester fluorene monomer, **1**, is occurring.

UV-vis absorption and photoluminescence spectra of the PF8BT dispersions show peak maxima at 469 and 542 nm, respectively (E and F, Figure 7) and exhibit PLQY values of 8.7–9.1%. Doubling the concentration of polymer in the dispersions had no effect on the optical properties of the nanoparticles.

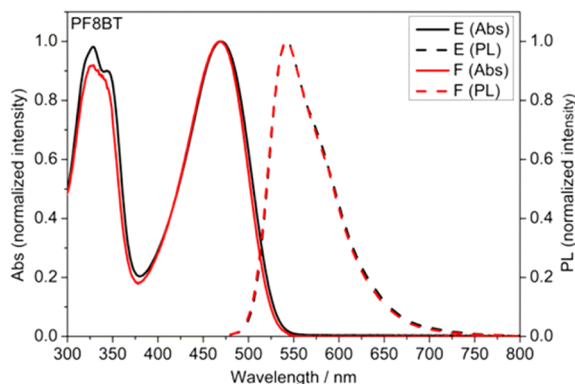


Figure 7. Absorption and photoluminescence spectra of PF8BT dispersions at 20 °C (E, F).

Poly(9,9-dioctylfluorene-*alt*-4-s-butylphenyldiphenylamine) (PF8TAA) Dispersions. Spherical nanoparticles were also prepared by the Suzuki–Miyaura coupling of equimolar amounts of monomers **1** and **4** (G and H, Table 1). The expected PF8TAA concentration in the nanoparticles is the same for both reactions and the standard reaction (G) produced a stable dispersion containing polymer of molar mass, $M_n = 19\,000 \text{ g mol}^{-1}$ exhibiting a z-average particle size, $d_z = 41 \text{ nm}$ ($\text{PDI} = 0.33$) by DLS. A 4-fold increase in the amount of monomers, xylene and surfactant present at start of the reaction (H), produced a lower molar mass polymer, $M_n = 9\,000 \text{ g mol}^{-1}$ but slightly larger particles by DLS ($d_z = 56 \text{ nm}$,

$\text{PDI} = 0.22$). TEM analysis of these PF8TAA dispersions revealed a homogeneous distribution of spherical particles (see Figure 8). The mean number-average particle diameters determined by TEM and DLS analysis are consistent within experimental error (G 19 and 18 nm, H 41 and 33 nm).

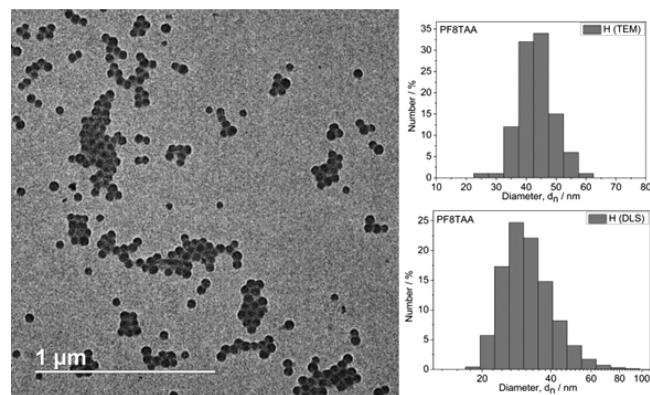


Figure 8. TEM image (left) of spherical nanoparticles present in PF8TAA dispersion (H). Right images are size distribution of the particles ($d_n = 41 (\pm 6)$ nm) obtained in TEM analysis (top) compared against number-average particle size distribution ($d_n = 33$ nm) of the dispersion obtained in DLS analysis (bottom).

The PF8TAA dispersions gave virtually identical absorption and photoluminescence (see Figure 9) with peak maxima at 388 and 435 nm and PLQY values of 3.4 and 5.2% respectively.

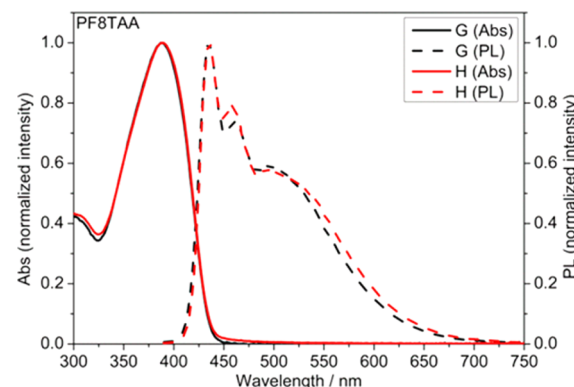


Figure 9. Absorption and photoluminescence spectra of PF8TAA dispersions at 20 °C (G, H).

Poly(9,9-dioctylfluorene-*alt*-bithiophene) (PF8T2) Dispersions. The Suzuki–Miyaura cross-coupling dispersion reaction was applied for the preparation of PF8T2, a polymer that is also known to assemble into ordered phases such as those seen for PF8. Reaction of equimolar amounts of monomers **1** and **5** gave rod-like nanoparticles (I and J, Table 1) of PF8T2 polymers with molar mass, $M_n = 12\,000\text{--}13\,000 \text{ g mol}^{-1}$.

DLS analysis of these dispersions suggested that the more concentrated conjugated polymer emulsion (J) produced larger nanoparticles ($d_z = 88 \text{ nm}$) with a relatively narrow particle size distribution ($\text{PDI} = 0.18$) in the context of these systems. TEM analysis of these dispersions revealed a homogeneous distribution of rod-like structures with reaction J showing larger, more uniform, rod-like nanoparticles (205 nm in length, with an aspect ratio of 4, Figure 10). The growth of similar

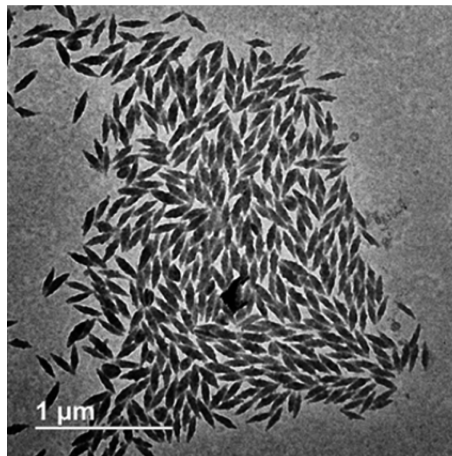


Figure 10. TEM image of nanoparticles present in PF8T2 dispersion (J). Regular rods, with dimensions of $205 (\pm 16)$ nm \times $52 (\pm 6)$ nm, equating to an aspect ratio of 4.

sized nanocrystals has been recently reported. These are grown from heated, concentrated solutions of PF8T2 in *p*-xylene that are cooled to room temperature.⁴⁰

Reaction J equates to a PF8T2 dispersion containing 8.2 mg mL^{-1} of conjugated polymer (Table 2). MALDI-TOF mass

Table 2. Optical Properties of Conjugated Polymer Nanoparticulate Dispersions

reaction	polymer concn ^a /mg mL ⁻¹	polymer concn in			$\Phi^e/\%$
		NP ^b /mg mL ⁻¹	$\lambda_{abs}^c/\text{nm}$	λ_{em}^d/nm	
A	PF8, 3.0	78	408, 442	441	21
B	PF8, 6.0	155	409, 442	440	25
C	PF8, 8.6	117	408, 441	440	22
D	PF8, 11.1	104	407, 441	440	23
E	PF8BT, 2.0	52	469	541	8.7
F	PF8BT, 4.0	105	468	543	9.1
G	PF8TAA, 2.6	69	387	434	3.4
H	PF8TAA, 9.5	69	389	435	5.2
I	PF8T2, 2.1	55	467	515, 557	2.8
J	PF8T2, 8.2	111	503	518, 556	5.1

^aApproximate conjugated polymer concentration of emulsion upon complete conversion. ^bConjugated polymer concentration in xylene in nanoparticles. ^c λ_{abs} : wavelengths of absorption maxima of emulsions diluted in water. ^d λ_{em} : wavelengths of emission maxima of emulsions diluted in water. ^ePhotoluminescence quantum yield (Φ). Results are average of at least three measurements. Errors of 10% associated with the values.

spectrometry of a low molar mass polymer fraction from the PF8T2 dispersions indicated chains terminated predominantly with hydrogen terminated fluorene units (see Supporting Information). Other distributions can be identified with F8-rich polymer structures suggesting some homocoupling of the boronic ester fluorene monomer, I. This would appear to be a major factor that prevents formation of even higher molar mass polymer in these aqueous dispersions.

UV/vis absorption spectra of the PF8T2 dispersions are presented in Figure 11. Dispersions from reaction I show a peak maximum at 467 nm whereas a dispersion derived from reaction J is red-shifted, exhibiting a peak maximum at 503 nm. Polymer chains in the larger rods of reaction J, produced at

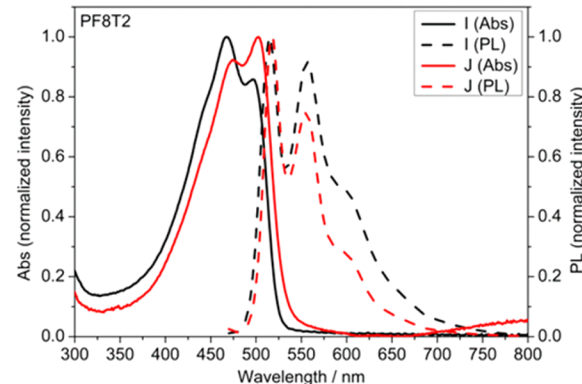


Figure 11. Absorption and photoluminescence spectra of PF8T2 dispersions at $20\text{ }^\circ\text{C}$ (I, J).

higher concentrations, may have greater interchain interactions over longer length scales.

This may explain the red-shift in the absorption spectrum when compared to that observed for the smaller rod-like nanoparticles evident for reaction I. The maxima in the emission spectra of the two dispersions more closely converge at $\lambda = 517$ and 557 nm , respectively. The absorption spectra of the PF8T2 in nanoparticles are very similar to those observed for the polymer deposited as a thin film.⁴¹ A comparison of the absorption spectra recorded for PF8T2 from reaction I as nanoparticles (dispersion), dissolved in THF (solution) and as a thin film are shown in Figure 12. PLQY (Φ) values of 2.8% and 5.1% were recorded for the PF8T2 emulsions created from reactions, I and J, respectively.

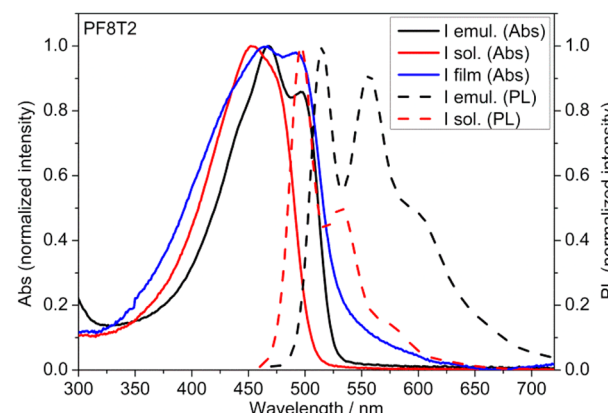


Figure 12. Absorption and photoluminescence spectra of PF8T2 polymer from reaction I in emulsion, dissolved in THF (solution) and as a film cast from dichlorobenzene solution, annealed at $80\text{ }^\circ\text{C}$ for 1 h.

CONCLUSIONS

In summary, we report the direct synthesis of conjugated polymer nanoparticles by the Suzuki–Miyaura reaction at room temperature to give high concentrations of conjugated polymer dispersed in water. These concentrations are commensurate with those of organic solutions employed for organic electronic device fabrication (ca. 10 mg mL^{-1}). Polymers such as PF8 and PF8T2 that can self-assemble into highly ordered phases give uniform distributions of anisotropic nanoparticles. By contrast, PF8BT and PF8TAA give homogeneous distributions of spherical nanoparticles. It appears that the major factor

governing nanoparticle size in these systems is the ratio of the organic phase to surfactant. Increasing the amount of xylene (above 2 mL) and Triton X-102 (above 5 wt %) always resulted in a small increase in the particle size of the polymer regardless of the type or the concentration of monomers used in the reaction. The ordering in the nanoparticles, particularly in the case of PF8, yielded PLQY (Φ) levels of 21–25%, values that are significant for this particular polymer in the solid state.

The room temperature emulsion polymerization can be applied to a wide range of suitably functionalized monomers and can deliver homogeneous dispersions of nanoparticles at high concentration of conjugated polymer. We are currently investigating the mechanism that underpins the unprecedented formation of the anisotropic nanoparticles, the self-assembly of these materials and their use for the fabrication of OFET, OPV, and photonic devices.

■ ASSOCIATED CONTENT

S Supporting Information

Intensity and number-average particle size distributions, TEM images of the remaining dispersions, cumulative fits to the absorption spectra of PF8 dispersions (reactions B–D) and MALDI–TOF mass spectra of examples of each polymer present in the dispersions. This material is available free of charge via the Internet at <http://pubs.acs.org>.

■ AUTHOR INFORMATION

Corresponding Authors

*E-mail: michael.turner@manchester.ac.uk. Fax: +44(0) 1612754273. Telephone: +44(0)1612754625.

*E-mail: andrew.foster@manchester.ac.uk.

Present Addresses

¹(D.M.) Center for Organic Electronic and Alternative Energy, Department of Chemistry and Center for Innovation in Chemistry, Faculty of Science, Ubon Ratchathani University, Warinchumrap, Ubon Ratchathani, 34190 Thailand.

[¶](M.-T.C.) Department of Chemistry, National Sun Yat-Sen University, No. 70, Lienhai Rd., Kaohsiung 80424, Taiwan.

[#](A.H.) Department of Physics and Energy, University of Limerick, Limerick, Ireland.

Notes

The authors declare no competing financial interest.

The findings in this paper are addressed in the patent application, P210170GB.

■ ACKNOWLEDGMENTS

D.M. would like to thank the Office of the Higher Education Commission, Thailand for supporting this research by grant fund under the program Strategic Scholarships for Frontier Research Network for the Joint Ph.D. Programme Thai Doctoral degree. A.B.F. would like to acknowledge funding from the Knowledge Centre for Materials Chemistry (KCMC). We thank Gareth Smith for his assistance in obtaining MALDI–TOF spectra of the polymers and Chris Muryn for help with formatting the TEM images.

■ REFERENCES

- Pecher, J.; Mecking, S. *Chem. Rev.* **2010**, *110*, 6260.
- Feng, L.; Zhu, C.; Yuan, H.; Liu, L.; Lv, F.; Wang, S. *Chem. Soc. Rev.* **2013**, *42*, 6620.
- Tuncel, D.; Demir, H. V. *Nanoscale* **2010**, *2*, 484.
- Hebner, T. R.; Wu, C. C.; Marcy, D.; Lu, M. H.; Sturm, J. C. *Appl. Phys. Lett.* **1998**, *72*, 519.

(5) Yang, Y.; Chang, S.-C.; Bharathan, J.; Liu, J. *J. Mater. Sci.: Mater. Electron.* **2000**, *11*, 89.

(6) Mori, K.; Ning, T.; Ichikawa, M.; Koyama, T.; Taniguchi, Y. *Jpn. J. Appl. Phys., Part 2: Lett.* **2000**, *39*, L942.

(7) Bao, Z.; Feng, Y.; Dodabalapur, A.; Raju, V. R.; Lovinger, A. J. *Chem. Mater.* **1997**, *9*, 1299.

(8) Szymanski, C.; Wu, C.; Hooper, J.; Salazar Mary, A.; Perdomo, A.; Dukes, A.; McNeill, J. *J. Phys. Chem. B* **2005**, *109*, 8543.

(9) Wu, C.; Szymanski, C.; McNeill, J. *Langmuir* **2006**, *22*, 2956.

(10) Fischer, C. S.; Baier, M. C.; Mecking, S. *J. Am. Chem. Soc.* **2013**, *135*, 1148.

(11) Landfester, K.; Montenegro, R.; Scherf, U.; Guntner, R.; Asawapirom, U.; Patil, S.; Neher, D.; Kietzke, T. *Adv. Mater. (Weinheim, Ger.)* **2002**, *14*, 651.

(12) Kietzke, T.; Neher, D.; Landfester, K.; Montenegro, R.; Guentner, R.; Scherf, U. *Nat. Mater.* **2003**, *2*, 408.

(13) Kietzke, T.; Stiller, B.; Landfester, K.; Montenegro, R.; Neher, D. *Synth. Met.* **2005**, *152*, 101.

(14) Landfester, K. *Angew. Chem., Int. Ed.* **2009**, *48*, 4488.

(15) Jenekhe, S. A.; Alam, M. M.; Zhu, Y.; Jiang, S.; Shevade, A. V. *Adv. Mater. (Weinheim, Ger.)* **2007**, *19*, 536.

(16) Mueller, K.; Klapper, M.; Muellen, K. *Macromol. Rapid Commun.* **2006**, *27*, 586.

(17) Baier, M. C.; Huber, J.; Mecking, S. *J. Am. Chem. Soc.* **2009**, *131*, 14267.

(18) Wang, R.; Zhang, C.; Wang, W.; Liu, T. *J. Polym. Sci., Part A: Polym. Chem.* **2010**, *48*, 4867.

(19) Sakamoto, J.; Rehahn, M.; Wegner, G.; Schlueter, A. D. *Macromol. Rapid Commun.* **2009**, *30*, 653.

(20) Negele, C.; Haase, J.; Leitenstorfer, A.; Mecking, S. *ACS Macro Lett.* **2012**, *1*, 1343.

(21) Chen, M.-T.; Vicic, D. A.; Turner, M. L.; Navarro, O. *Organometallics* **2011**, *30*, 5052.

(22) Guest, D.; Chen, M.-T.; Tizzard, G. J.; Coles, S. J.; Turner, M. L.; Navarro, O. *Eur. J. Inorg. Chem.* **2014**, *13*, 2200.

(23) Chen, M.-T.; Vicic, D. A.; Chain, W. J.; Turner, M. L.; Navarro, O. *Organometallics* **2011**, *30*, 6770.

(24) Nguyen, T.-Q.; Martini, I. B.; Liu, J.; Schwartz, B. J. *J. Phys. Chem. B* **2000**, *104*, 237.

(25) Noriega, R.; Rivnay, J.; Vandewal, K.; Koch, F. P. V.; Stingelin, N.; Smith, P.; Toney, M. F.; Salleo, A. *Nat. Mater.* **2013**, *12*, 1038.

(26) Schwartz, B. J. *Annu. Rev. Phys. Chem.* **2003**, *54*, 141.

(27) Wu, C.; McNeill, J. *Langmuir* **2008**, *24*, 5855.

(28) Wu, C.; Bull, B.; Szymanski, C.; Christensen, K.; McNeill, J. *ACS Nano* **2008**, *2*, 2415.

(29) Behrendt, J. M.; Wang, Y.; Willcock, H.; Wall, L.; McCairn, M. C.; O'Reilly, R. K.; Turner, M. L. *Polym. Chem.* **2013**, *4*, 1333.

(30) Behrendt, J. M.; Foster, A. B.; McCairn, M. C.; Willcock, H.; O'Reilly, R. K.; Turner, M. L. *J. Mater. Chem., C: Mater. Opt. Electron. Devices* **2013**, *1*, 3297.

(31) Ong, B. S.; Wu, Y.; Liu, P.; Gardner, S. *Adv. Mater. (Weinheim, Ger.)* **2005**, *17*, 1141.

(32) Kuehne, A. J. C.; Gather, M. C.; Sprakler, J. *Nat. Commun.* **2012**, *3*, 2085/1.

(33) Yang, Z.; Huck, W. T. S.; Clarke, S. M.; Tajbakhsh, A. R.; Terentjev, E. M. *Nat. Mater.* **2005**, *4*, 486.

(34) Liu, C.; Wang, Q.; Tian, H.; Liu, J.; Geng, Y.; Yan, D. *J. Phys. Chem. B* **2013**, *117*, 8880.

(35) Liu, C.; Wang, Q.; Tian, H.; Liu, J.; Geng, Y.; Yan, D. *Macromolecules* **2013**, *46*, 3025.

(36) Ariu, M.; Lidzey, D. G.; Bradley, D. D. C. *Synth. Met.* **2000**, *111*–112, 607.

(37) Knaapila, M.; Bright, D. W.; Stepanyan, R.; Torkkeli, M.; Almasy, L.; Schweins, R.; Vainio, U.; Preis, E.; Galbrecht, F.; Scherf, U.; Monkman, A. P. *Phys. Rev. E* **2011**, *83*, 051803/1.

(38) Bansal, A. K.; Ruseckas, A.; Shaw, P. E.; Samuel, I. D. W. *J. Phys. Chem. C* **2010**, *114*, 17864.

(39) Khan, A. L. T.; Sreearunothai, P.; Herz, L. M.; Banach, M. J.; Kohler, A. *Phys. Rev. B* **2004**, *69*, 085201/1.

- (40) Werzer, O.; Resel, R.; Chernev, B.; Plank, H.; Rothmann, M. M.; Strohriegl, P.; Trimmel, G.; Rapallo, A.; Porzio, W. *Polymer* **2011**, *S2*, 3368.
- (41) Lim, E.; Jung, B.-J.; Shim, H.-K. *Macromolecules* **2003**, *36*, 4288.